Supplementary Information

Formation of Ag$^+$-N-TiO$_2$ Nanochains and Their HPA-Composites as Highly Visible Light-Sensitive Photocatalysts toward Two-Color Solar Cells

Hyungjoo Lee, Jina Lee, Yang-Hwa Lee,   Jooran Lee,   and Minjoong Yoon*

Molecular/Nano Photochemistry & Photonics Lab, Department of Chemistry, Chungnam National University, 79 Daehak-ro, Yuseong-gu,   Daejeon, 305-764 (Republic of Korea)

* Address correspondence to mjyoon@cnu.ac.kr.

Experimental Details

Formation and characterization of Ag$^+$-N-TiO$_2$ nanochains and their HPA composites: First of all, N-TiO$_2$ nanoparticles were synthesized by sol-gel method and hydrothermal method.   4mL aqueous solution of 2 M NH$_4$OH was dropped slowly for 5 min to aqueous 300 mL of 10 mM (NH$_4$)$_2$TiO(C$_2$O$_4$)$_2$ solution and stirred at room temperature. After 1hr, the solution was changed from sol to gel. It was filtered to obtain hard gel as precursor, and then washed with distilled water of 2,000 mL. In order to get pure product, the gel precursor was added distilled water (100 mL), followed by sonication for 10 min in an ultrasonic bath (Fisher Scientific model FS20, 70 W, 42 kHz) and repeated washing procedure. The 100 ml gel precursor was heated at 200°C for 6 hrs in an autoclave. After being cooled to room temperature, the product was filtered and dried in vacuum oven at 200°C for 5 hrs, being identified to be N-TiO$_2$ nanoparticles.   The prepared N-TiO$_2$ nanoparticles (0.10 mM) were mixed with 0.15M AgNO$_3$ solution of 10mL by stirring at room temperature for 2 days in the dark.   The mixture was evaporated by heating at 100°C for 12 hrs until the remaining about 20mL and dried in oven for 1 day. The dried

solids were ground in an agate mortar and calcined at 400°C for 6 hrs. As a result, the Ag^+-N-TiO_2 nanochains were obtained.

Surface analysis of the synthesized Ag^+-N-TiO_2 nanochains was performed by using XPS spectroscopy. The XPS spectra of the Ag^+-N-TiO_2 nanochains were measured by using a Multilab ESCA 2000 fitted with an Mg KR source (1253.6 eV) with two ultra-high-vacuum (UHV) chambers, one for sample preparation and the other for analysis. The anode was operated at 120 W (10 mA and 12kV), and the analyzer was operated at a constant narrow scan pass energy of 30 eV. The analysis area was 2 × 3 mm. The photoelectrons were collected at an electron takeoff angle of 55°. The binding energy shifts due to surface charging were corrected using the C 1s core level at 285 eV as an internal standard. Figure S-1 shows the X-ray photoelectron spectra (XPS) of (A) $Ti_{2p\,(1/2,\,3/2)}$, (B) N_{1s}, and (C) O_{1s} core levels recorded from a pellet of Ag^+-N-TiO_2 nanochains powder. The XPS peaks were assumed to have Gaussian line shapes and were resolved into individual components by a nonlinear least-squares procedure after proper subtraction of the baseline. Ti_{2p} spectrum was analyzed to be originated from four binding energies of O-Ti-N (458.8 eV), Ti-N (460.35 eV), TiO_2 (464 eV) and TiO_2 (465 eV) while N 1s spectrum revealed binding energies O-Ti-N (399.2 eV) and above O-Ti-N (401.2 eV). The O 1s peak was resolved into three peaks at TiO_2 (529.05 eV), O-Ti-N (530.66 eV) and O-Ti-N (531.97 eV). The XPS of Ag 3d was also observed to resolved into binding energy from two peaks at Ag_2O (367.68 eV) and Ag-O (368.25 eV).[S-1] These results indicate that nitrogen is doped into TiO_2 by binding with Ti lattice whereas Ag ion is bound with oxygen on the surface of TiO_2.

The heteropolytungstic phosphoric acid (HPA) composite of Ag^+-N-TiO_2 nanochains was formed simply by mixing Ag^+-N-TiO_2 nanochains (0.05 M) with HPA (0.5 mM) in aqueous solution. The HPA-incorporation with Ag^+-N-TiO_2 was confirmed as proved by measuring FT-IR spectrum of as-prepared HPA/ Ag^+-N-TiO_2 (Fig. S-2), which showed the red-shifts in vibrational frequency bands of W-O (750-900 cm^{-1} region) as compared to those reported for free HPA.[21]

Measurements of photocatalytic activities and quantum yields: A 10 mg portion of Ag^+-N-TiO_2 nanochains, N-TiO_2 particles, or Degussa P-25 was mixed with 8 mL of the aqueous MO solution (5 ×

10^{-5} M) in optically matched Pyrex test tubes, and the mixed solutions were simultaneously irradiated in the Hanovia medium pressure Mercury lamp (450 W). After a certain period of irradiation, each solution was centrifuged to sediment the photocatalysts, followed by taking the supernatant solution to measure the absorption spectral change of MO to monitor the photooxidation. The irradiation lamp was set inside the air-circulating house so that it can be cooled during irradiation. The lamp housing was placed next to the reaction vessel attached to a cut-off filter to remove the light with wavelength shorter than 400 nm and 500 nm. The distance between the sample vessel and the lamp was adjusted so that the incident power of lamp was 0.5 W.   Figure S-3 shows the UV-Visible absorption spectra of 8 mL MO solution measured as a function of irradiation with visible light (>400 nm) in the presence of 10 mg of P-25, N-TiO$_2$ nanoparticles and Ag$^+$-N-TiO$_2$ nanochains with oxygen bubbling. Upon irradiation of the aqueous solution of MO in the presence of P-25 (Figure S-3(A)) and N-TiO$_2$ nanoparticles (Figure S-3(B)), intensity of the 465 nm band was slightly decreased whereas MO itself was confirmed to be photochemically inert as observed by no change in the absorption spectrum upon irradiation, indicating slight photocatalytic oxidation of MO.   However, in the presence of Ag$^+$-N-TiO$_2$ nanochains (Figure S-3(C)), the absorption spectrum of MO was observed to be disappeared upon a 4 hours of irradiation, indicating that MO is almost completely decomposed.   Figure S-4 shows the plot of the absorbance change of MO in the presence of different photocatalysts as a function of illumination time.

The photocatalytic quantum yields were measured by chemical actinometry using ferri-oxalate actinometer (a solution of complex salt K$_3$[Fe(C$_2$O$_4$)$_3$] in sulfuric acid)   which is known to be photochemically active after excitation with ultraviolet and visible lights[S-3] and undergoes the accepted overall reaction (1) : [S-4]

$$2[Fe(III)(C_2O_4)_3]^{3-} + h\nu \rightarrow 2[Fe(II)(C_2O_4)_2]^{2-} + C_2O_4 + 2CO_2 \uparrow \qquad (1)$$

In general, the radiation intensity is

$$I \text{ (photons/s)} = n_{Fe(II)} / \Phi_\lambda t_r (1 - 10^{-D(\lambda)}) \qquad (2)$$

3

where $n_{Fe(II)}$ is the number of particles that have absorbed a photon in the solution of volume V; t_r, s, is the phototransformation time for this amount of substance; Φ_λ is the wavelength-dependent quantum yield in the reaction Fe(III) $\rightarrow$ Fe(II); and $D(\lambda)$ is the optical density of the solution. Incidentally,

$$n_{Fe(II)} = CVN_A \tag{3}$$

where C (moles/cm^3) is the initial Fe(III) concentration; V, cm^3, is the solution volume; and $N_A = 6.023 \times 10^{23}$ is Avogadro's number. When the solution heavily absorbs light (which is achieved by properly selecting the cell thickness and concentration of the photoactive substance), the value of $10^{-D(\lambda)}$ in Eq. (2) may be neglected with a small error in comparison with Eq. (1). Hence,

$$\text{(photon/s)} = n_{Fe(II)} / \Phi_\lambda t_r \tag{4}$$

The absolute quantum yield Φ_λ was calculated by measuring I (photons/s).[S-5]

We prepared potassium ferrioxalate (K$_3$[Fe(C$_2$O$_4$)$_3$]•3H$_2$O) by 1.5 M K$_2$C$_2$O$_4$ solution and 1.5 M FeCl$_3$ solution (3 : 1). A monochromator of 3 mW Hg Arc lamp was used for measurement of light intensity. Mixed solution of 5.5ml (potassium ferrioxalate solution 4ml, acetate buffer 1ml, phenanthroline solution 0.5ml) was exposed in light for 60min. Therafter, we measured the difference of absorption at 510nm by using UV-visible spectrometer. Figure S-5 shows (A) absorption spectral change of ferroxalate as a function of visible light irradiation time in the presence of the Ag$^+$-N-TiO$_2$ nanochains with 436 nm monochromator, (B) absorption spectral change of methyl orange oxidation as a function of visible light (436 nm) irradiation time in the presence of the Ag$^+$-N-TiO$_2$ nanochains and (C) the quantum yield of several photocatalysts. Number of Fe(II) ($n_{Fe(II)}$) is 1.89×10^{17}. I (photons/s) is 3.12×10^{15} / min. And $n_{Ag^+\text{-N-TiO2}}$ is 9.2×10^{16}; $n_{Fe(II)} = \{(6.023 \times 10^{23}) \times (5.5 \times 10^{-3}\ \text{L}) \times (0.63389)\}$ / $\{(1.11 \times 10^4\ \text{M}^{-1}\ \text{cm}^{-1}\} \times 1\ \text{cm}\} = 1.89 \times 10^{17}$; I (photons/s) $= n_{Fe(II)} / \Phi_\lambda t_r = 1.89 \times 10^{17} / 1.01 \times 60\ \text{min}$ $= 3.12 \times 10^{16}$ / min; $n_{Ag^+\text{-N-TiO2}} = \{(6.023 \times 10^{23}) \times (8 \times 10^{-3}\ \text{L}) \times (0.40092)\}$ / $\{(2.1 \times 10^4\ \text{M}^{-1}\ \text{cm}^{-1}\} \times 1\ \text{cm}\} = 9.2 \times 10^{16}$. Thus, quantum yield of the photocatalytic degradation of Methyl Orange using Ag$^+$-N-TiO$_2$ nanochains was estimated to be 0.49 (49%) as follows, which was extremely higher than P-25 (3 %) and N-TiO$_2$ (9%) as seen below

$$\Phi_{Ag^+\text{-N-TiO2}} = n_{Ag^+\text{-N-TiO2}} / \text{I (photons/s)} = (9.2 \times 10^{16}) / (3.12 \times 10^{16}\ /\text{min} \times 60\ \text{min}) = 0.49$$

Surface characterization of different Ag⁺-N-TiO₂ electrode films: Figure S-6 shows the typical SEM images of the electrodes of Ag^+-N-TiO_2 nanoparticles and HPA-incorporated N-TiO_2 nanochains. The white crystalline particles of HPA were formed as islands upon incorporation with the nanochains. Figure S-7 shows the XRD pattern recorded for the HPA-incorporated nanochains on an FTO glass surface and the data were recorded at the 2θ range of (20-60) respectively. The XRD peaks were analyzed into anatase N-TiO_2 nanopartlcles exhibiting the (010), (004), (200), (105), (204) planes (■).[S-2] The peaks (●,★) can be indexed to the FTO glass and Ag ((111), (200)), respectively. The peaks (▲) can be indexed to the triclinic of WO_3 (1966, Roth, Waring. *J. Res. Natl. Bur. Stand.*, set. A, 70281. a = 7.384, b = 7.512, c = 3.846),[S-3] confirming that nanochains were heterojunctioned with HPA.

References

[S-1] Xin, B.; Jing, L.; Ren, Z.; Wang, B.; Fu, H.   *J. Phys. Chem. B* **2005**, *109,* 2805.

[S-2] Xe, L.; Xu, N.; Fang, H.   *J. Sol-Gel Sci. Tech.* **2005**, *40*, 65.

[S-3] Parker, C. A. *Proc. R. Soc. London, Ser. A.* **1953**, *220*, 104.

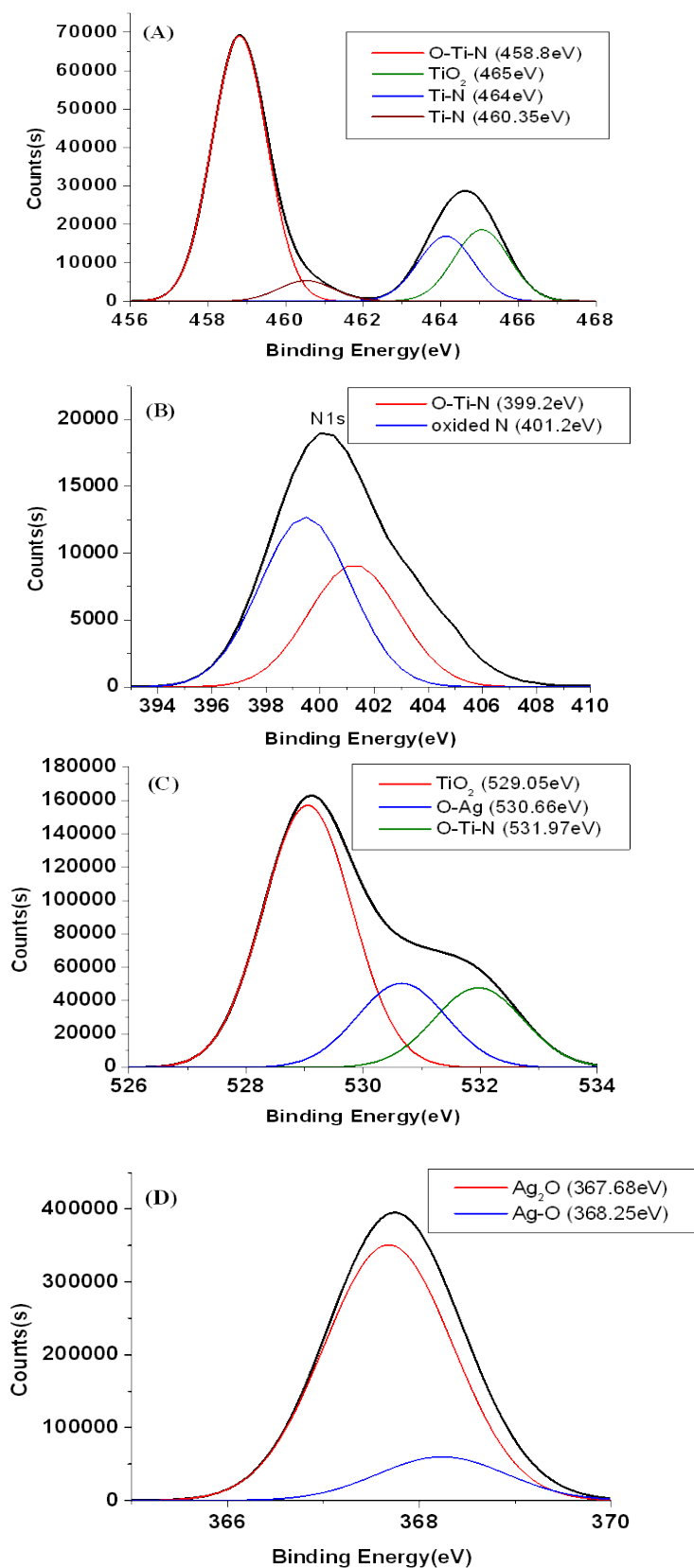[S-4] Parker, C. A.; Hatchard, C. G. *J. Phys. Chem.* **1959**, *63*, 22.

Figure S-1. X-ray photoelectron spectra of (A) $Ti_{2p (1/2, 3/2)}$, (B) N_{1s}, (C) O_{1s} and (D) Ag_{3d} in Ag^+-N-TiO_2 nanochains.
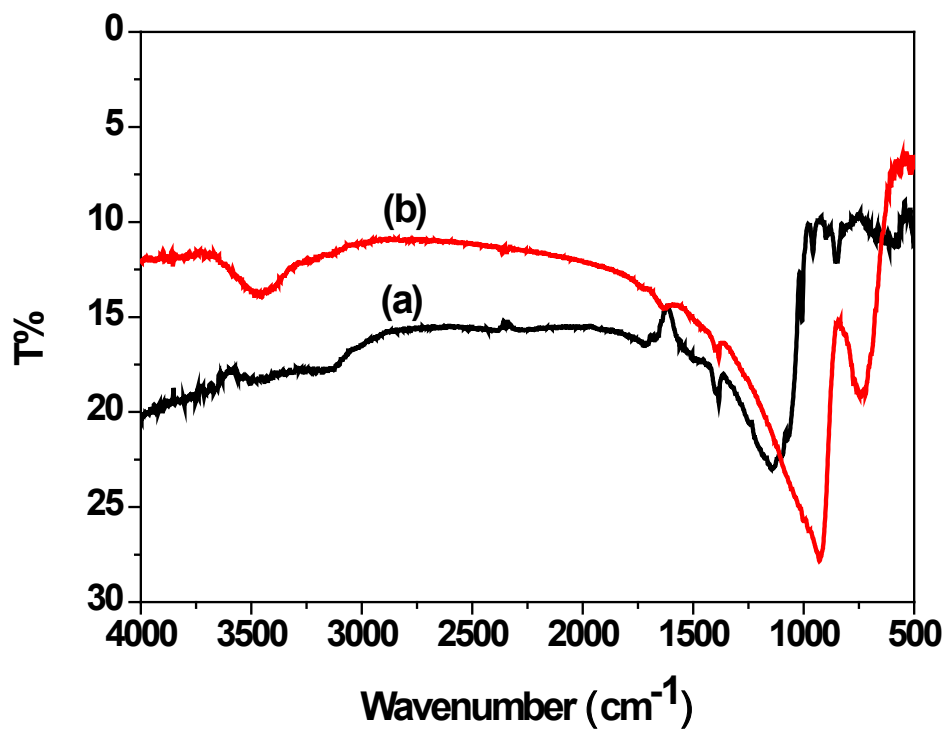
Figure S-2. FT-IR spectra of (a) free Ag^+-N-TiO_2 (b) Ag^+-N-TiO_2/HPA.
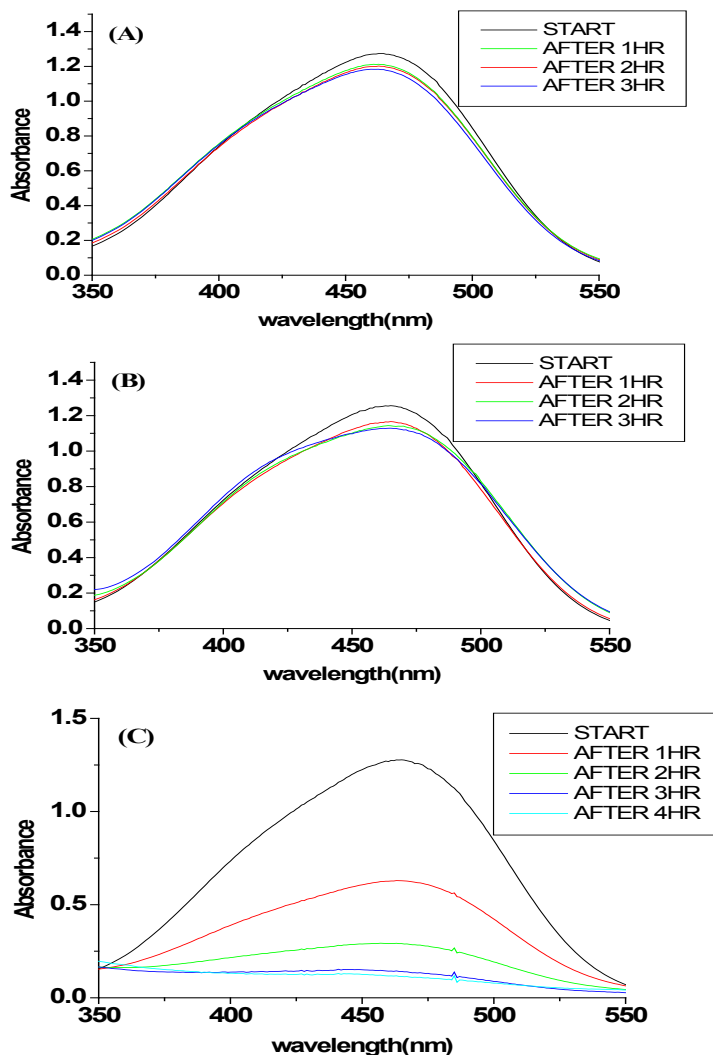
Figure S-3. Absorption spectral change of methyl orange as a function of visible light irradiation time in the presence of (A) P-25 TiO$_2$, (B) the N-TiO$_2$ nanopartlcles and (C) the Ag$^+$-N-TiO$_2$ nanochains with 400 nm cut-off filter.
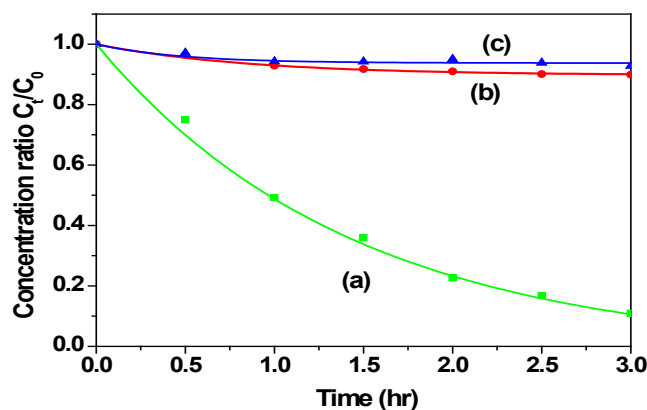
Figure S-4. Plot of the concentration change of methyl orange oxidation as a function of visible light irradiation time in the presence of the Ag$^+$-N-TiO$_2$ nanochains (a), the N-TiO$_2$ nanoparticles (b) and P-25 TiO$_2$ (c). The irradiation light was spectrally use with 400 nm cut-off filter.
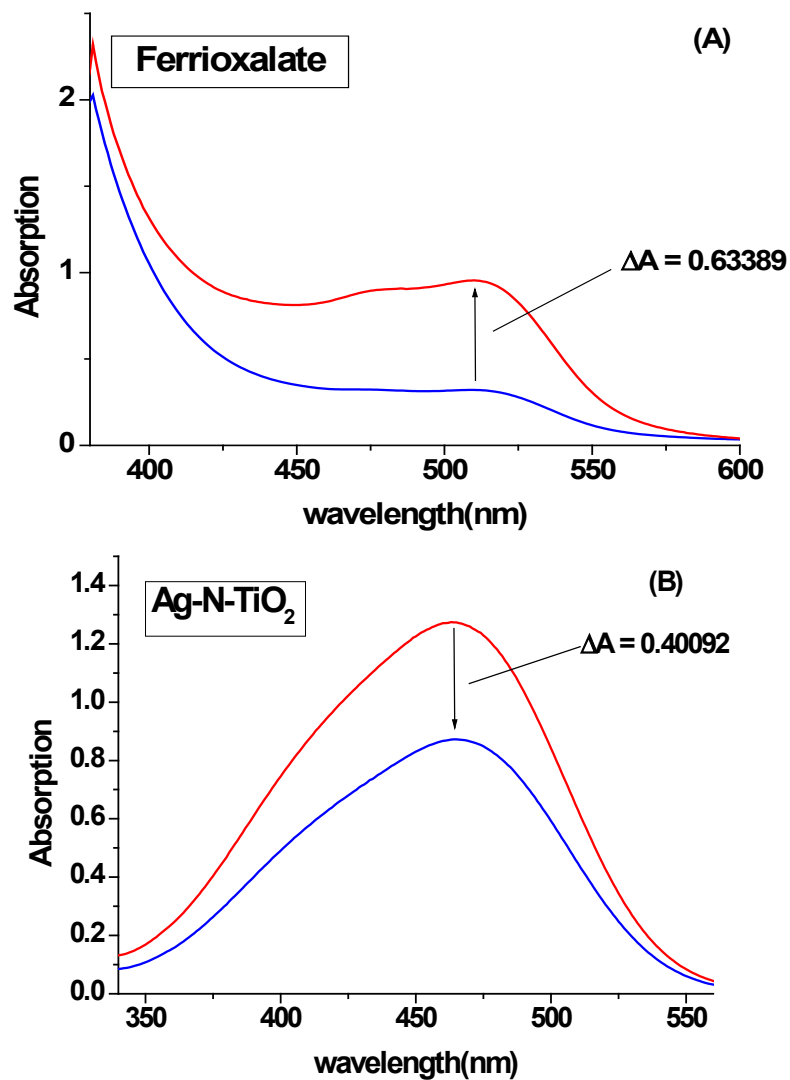
8

Figure S-5. (A) Absorption spectral change of ferroxalate as a function of visible light irradiation time in the presence of the Ag^+-N-TiO_2 nanochains with 436 nm monochromator (B) Absorption spectral change of methyl orange oxidation as a function of visible light irradiation time in the presence of the Ag^+-N-TiO_2 nanochains with 436 nm monochromator.
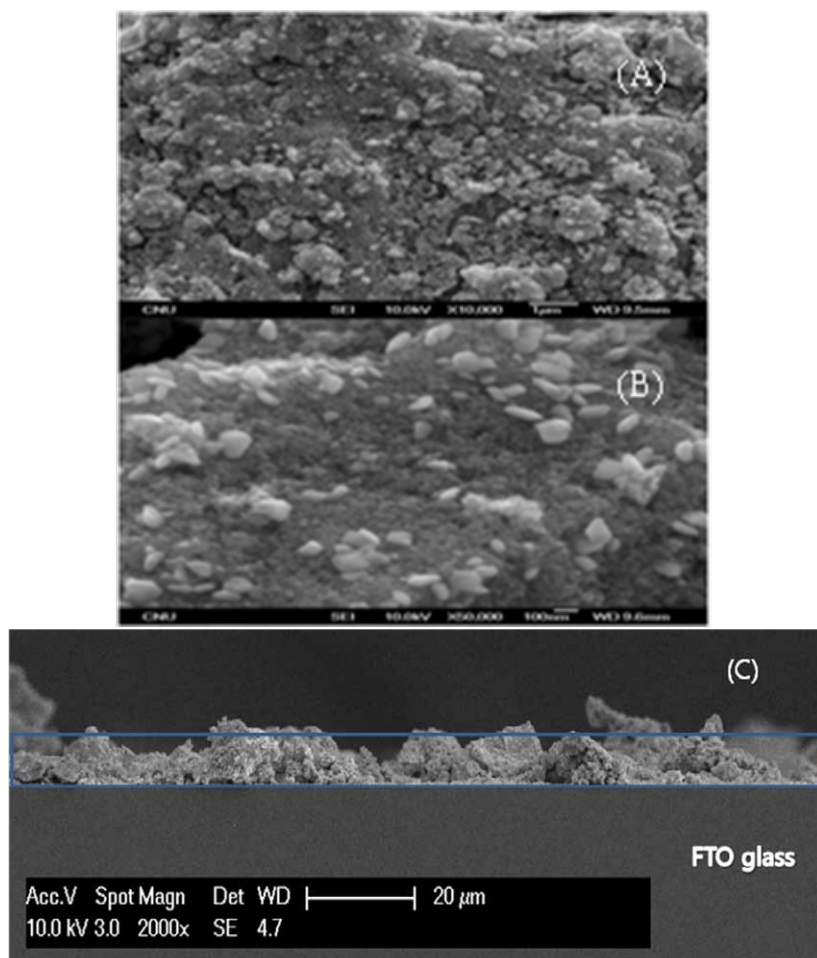
Figure S-6. SEM images of surface (scale bar (A) 1μm, (B) 100nm) and cross section of HPA-Ru-dyes-Ag^+ −N-TiO$_2$ nanoparticle (C).
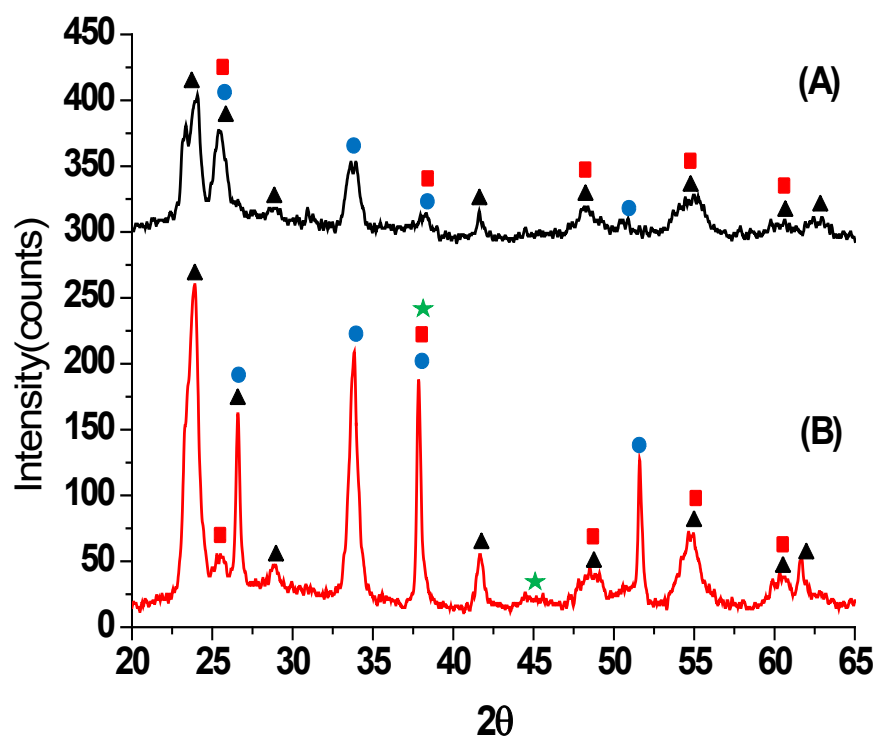
Figure S-7. X-ray diffractions of HPA-N-TiO$_2$ nanoparticles electrode (A) and HPA-Ag$^+$-N-TiO$_2$ nanochains electrode (B) (▲- WO$_3$, ●- FTO, ■- N-TiO$_2$, ★- Ag).